D1-82-0167

BOEING SCIENTIFIC RESEARCH LABORATORIES

Thrust Programs for Minimum Propellant Consumption During Vertical Take-Off and Landing Maneuvers of a Rocket Vehicle in a Vacuum

David G. Hull

July 1962

D1-82-0167

BOEING SCIENTIFIC RESEARCH LABORATORIES

FLIGHT SCIENCES LABORATORY TECHNICAL REPORT NO. 59

THRUST PROGRAMS FOR MINIMUM PROPELLANT CONSUMPTION DURING VERTICAL TAKE-OFF AND LANDING MANEUVERS OF A ROCKET VEHICLE IN A VACUUM

DAVID G. HULL

JULY 1962

TABLE OF CONTENTS

Summary

List of symbols

1. Introduction

2. Miele's theory for the extremization of linear integrals

3. Vertical flight in a uniform gravitational field

    3.1. Class of admissible displacements

    3.2. Region of admissible paths

    3.3. Composition of the extremal arc

    3.4. Take-off

    3.5. Landing

4. Vertical flight in an inverse square law gravitational field

    4.1. Take-off

    4.2. Landing

5. Vertical flight in an arbitrary gravitational field

Conclusions

References

Appendix A. The admissible domain

Appendix B. Analysis of comparison programs

THRUST PROGRAMS FOR MINIMUM PROPELLANT CONSUMPTION DURING VERTICAL TAKE-OFF AND LANDING MANEUVERS OF A ROCKET VEHICLE IN A VACUUM

by

DAVID G. HULL(*)

BOEING SCIENTIFIC RESEARCH LABORATORIES

SUMMARY

In this paper the thrust programs for minimum propellant consumption during vertical take-off and landing maneuvers of a rocket in a vacuum are derived, first for a uniform gravitational field, then for the inverse square law gravitational field. It is shown that, regardless of the mathematical form of the attracting force, the extremal arc for take-off is composed of a maximum thrust subarc followed by a coasting subarc, and the extremal arc for landing is composed of a coasting subarc followed by a maximum thrust subarc.

(*) Staff Associate, Astrodynamics and Flight Mechanics Group.

LIST OF SYMBOLS

g = Acceleration of gravity (ft sec^{-2})

h = Altitude (ft)

m = Instantaneous mass (lb ft^{-1} sec^{2})

r_o = Radius of the attracting body (ft)

t = Time (sec)

u = Nondimensional velocity

V = Velocity (ft sec^{-1})

α = Modulus of the nondimensional acceleration

β = Propellant mass flow (lb ft^{-1} sec)

ϵ = Nondimensional total energy

ζ = Propellant mass ratio

η = Nondimensional altitude

θ = Nondimensional time

ρ = Nondimensional distance from the center of attraction

μ = Nondimensional mass

τ = Ratio of the thrust to the weight evaluated at the surface of the attracting body

ω = Fundamental function

Subscripts

c = Burnout point

f = Final point

d = Firing point

E = Equivalent exit condition of the rocket engine

i = Initial point

o = Surface of the attracting body

1. INTRODUCTION

This paper is concerned with the determination of the thrust programs which yield the minimum propellant consumption for vertical take-off and landing maneuvers in a vacuum. First, in order to gain some insight into the problem, it is assumed that flight takes place in a uniform gravitational field. After this, the more general problem of the inverse square law gravitational field is analyzed.

Once the compositions of the optimum take-off and landing trajectories are determined, the equations of motion are integrated, when possible, and the characteristics of these paths (burnout velocity and altitude for take-off, firing velocity and altitude for landing, and the amount of propellant consumed during each maneuver) are discussed.

The optimization technique used in this analysis is that developed by Miele in Ref. 1 for the extremization of linear integrals.

2. MIELE'S THEORY FOR THE EXTREMIZATION OF LINEAR INTEGRALS

The method used in this paper for determining optimum thrust programs is that developed in Ref. 1. This method is concerned with the extremization of an integral which is linear in the derivative of an unknown function y(x), that is, an integral of the form

$$I = \int_i^f \left[\varphi(x,y)\, dx + \psi(x,y)\, dy\right] \tag{1}$$

where the functions φ and ψ are given and where the symbols i and f denote initial and final points, respectively. It is required that the class of admissible paths be contained in a region which is bounded by a closed curve and that the prescribed end-points belong to the boundary of this region. Once these conditions are met, the extremal arc--that particular curve y(x) which maximizes or minimizes the integral--can be determined by examining the properties of the fundamental function which is defined as (Ref. 1)

$$\omega(x,y) = \frac{\partial \psi}{\partial x} - \frac{\partial \varphi}{\partial y} \tag{2}$$

Several classes of extremal problems exist depending on the sign distribution of the fundamental function within the admissible domain. However, since the sign of the fundamental function is constant in the problems which follow, only the results for that part of the theory are presented. Specifically, Ref. 1 shows that (a) the extremal arc lies on the boundary of the admissible domain ICFDI of Fig. 1 and (b) the sense in which it is

traveled depends on the sign of the fundamental function and whether a maximum or a minimum value is desired for the integral. If the fundamental function is positive everywhere, the following results are valid: (a) the path ICF, which is traveled in such a way that the admissible domain is always on the left, maximizes the integral; and (b) the path IDF, which is traveled in such a way that the admissible domain is always on the right, minimizes the integral. On the other hand, if the fundamental function is negative, maximum paths are transformed into minimum paths and vice verse (see Table 1).

TABLE 1

COMPOSITION OF THE EXTREMAL ARC

Fundamental function	Extremal arc	Type of Extremum
$\omega > 0$	ICF IDF	maximum minimum
$\omega < 0$	ICF IDF	minimum maximum

3. VERTICAL FLIGHT IN A UNIFORM GRAVITATIONAL FIELD

In this section, vertical flight in a vacuum is considered under the assumption that the gravitational field is uniform. The relevant equations are given by

$$\frac{dh}{dt} = \pm V \tag{3}$$

$$\frac{dV}{dt} = \pm \frac{\beta V_E}{m} \mp g_o \tag{4}$$

$$\frac{dm}{dt} = -\beta \tag{5}$$

where h is the altitude, V the velocity, β the propellant mass flow, V_E the constant equivalent exit velocity, m the mass, g_o the acceleration of gravity, and t the time. The upper signs are valid for ascending flight, while the lower signs are valid for descending flight with the tail of the vehicle pointed toward the attracting body.

It is recalled that the number of degrees of freedom of a differential system is the difference between the number of dependent variables and the number of equations. Also, it is observed that this system of three equations involves one independent variable (t) and four dependent variables (h, V, m, β), so that one degree of freedom exists. Consequently, some optimum requirement can be imposed on the flight path; in this case, it is desired that the burning program $\beta(t)$ be such that the propellant consumed during take-off or landing is a minimum. However, there exist limitations to the choice of this program, in that the rocket engine can

only develop instantaneous mass flows between a lower limit and an upper limit. If it is assumed that the lower limit is zero, the following inequality must be satisfied at all points of the flight path:

$$0 \leq \beta \leq \beta_{max} \tag{6}$$

Combining Eqs. (3) through (5), one obtains the differential relationship

$$d \log m = \mp \frac{dV}{V_E} \mp \frac{g_o dh}{V_E V} \tag{7}$$

If it is observed that $m_f/m_i = 1 - \zeta$, where ζ is the ratio of the propellant mass to the initial mass, the propellant required to transfer the rocket from an initial state V_i, h_i to a final state V_f, h_f is given by the linear integral

$$\log (1-\zeta) = \int_i^f \left[\mp \frac{dV}{V_E} \mp \frac{g_o dh}{V_E V} \right] . \tag{8}$$

which depends on the integration path h(V). Since log $(1-\zeta)$ is a maximum when ζ is a minimum, the problem of determining the burning program for minimum propellant consumption is formulated as follows: In the class of functions h(V) which satisfy the prescribed end-values for the velocity and the altitude and which are consistent with inequality (6), determine that particular function which maximizes the integral (8).

3.1. Class of Admissible Displacements

Before the theory can be applied to this linear integral, it is necessary to ascertain the existence of a region which contains all of the admissible paths. In this connection, consider the ascending flight of a rocket which, at a given time instant, has a velocity V and an altitude h, and let P be its position in the velocity-altitude plane (Fig. 2). After an infinitesimal time increment dt, the velocity becomes $V' = V + dV$, and the altitude becomes $h' = h + dh$, so that the position of the rocket is now represented by the point P'. Hence, the vector $\overline{PP}'$ is the infinitesimal displacement of the rocket in the Vh-plane. From the equations of motion, it is seen that the velocity and altitude increments are given by

$$dV = \left[\frac{\beta V_E}{m} - g_o\right] dt \qquad (9)$$

$$dh = V\,dt \qquad (10)$$

so that, for each mass flow β, there exists one infinitesimal displacement $\overline{PP}'$. However, because of the inequality (6), not every displacement is physically possible in that the class of admissible displacements from a point P is bounded by two limiting conditions: a displacement $\overline{PQ}$ corresponding to zero burning rate and a displacement $\overline{PR}$ corresponding to the maximum burning rate. In order to be absolutely certain that the region A contains all of the admissible displacements from the point P, consider an arbitrary displacement to each of the regions B, C, and D. A displacement to the region B is impossible, since this would require a negative mass flow. A displacement to the region C is also impossible,

since a mass flow greater than the maximum would be required. Finally, displacements to the region D are eliminated by the kinematic relation which states that, if the velocity is positive, there can be no decrease in the altitude. Hence, the region A contains all of the displacements which are physically possible for the rocket vehicle. Incidentally, the analysis for descending flight is entirely similar, and the limiting displacements are the images of $\overline{PQ}$ and $\overline{PR}$ with respect to point P (see Fig. 3).

3.2. Region of Admissible Paths

In the previous section, it has been shown that all physically possible displacements from a point are bounded by $\beta = 0$ and $\beta = \beta_{max}$ displacements. In a similar manner, it can be shown that all physically possible displacements to a point are bounded by $\beta = 0$ and $\beta = \beta_{max}$ displacements. Consequently, if this process of displacements is carried out throughout the Vh-plane, it is seen that the two curves $\beta = 0$ and $\beta = \beta_{max}$ which originate at the initial point and the two curves $\beta = 0$ and $\beta = \beta_{max}$ which terminate at the final point compose the boundary ICFDI of the region of admissible paths (see Fig. 4 for ascending flight and Fig. 5 for descending flight), that is, the region containing all of the trajectories which satisfy the prescribed end-values for the velocity and altitude as well as the inequality constraint (6). There exists no physically possible path which crosses the boundary of this region as is shown in Appendix A.

3.3. Composition of the Extremal Arc

This problem now meets all of the requirements of a linear problem, so

that Miele's theory is applicable. In this connection, the fundamental function is given by

$$\omega(V,h) = \pm \frac{g_o}{V_E V^2} \tag{11}$$

and, therefore, is positive for ascending flight and negative for descending flight. Since the thrust of a rocket engine is proportional to the mass flow, the optimum ascending path ICF includes a maximum thrust subarc followed by a zero thrust subarc (Fig. 4), while the optimum descending path IDF includes a zero thrust subarc followed by a maximum thrust subarc (Fig. 5).

3.4. Take-Off

In order to study the main characteristics of the extremal arc for take-off, it is convenient to introduce the nondimensional variables

$$\eta = \frac{hg_o}{V_E^2} \quad , \quad u = \frac{V}{V_E} \quad , \quad \mu = \frac{m}{m_i} \quad , \quad \tau = \frac{\beta V_E}{mg_o} \quad , \quad \theta = \frac{tg_o}{V_E} \tag{12}$$

and rewrite the equations of motion in the form

$$\frac{d\eta}{d\theta} = u \tag{13}$$

$$\frac{du}{d\theta} = \tau - 1 \tag{14}$$

$$\frac{d\mu}{d\theta} = -\tau\mu \tag{15}$$

For the subarc flown with maximum thrust, the thrust-to-weight ratio τ and the nondimensional mass μ satisfy the relationship

$$\tau = \frac{\tau_i}{\mu} \quad , \quad \tau_i = \frac{\beta_{max} V_E}{m_i g_o} \tag{16}$$

so that, after the time is eliminated, the integration process leads to the results

$$u + \log \mu - \frac{\mu}{\tau_i} = C_1 \tag{17}$$

$$\eta + \frac{\mu}{\tau_i}(1+C_1 - \log \mu) + \frac{\mu^2}{2\tau_i^2} = C_2 \tag{18}$$

On the other hand, for coasting flight the thrust-to-weight ratio is $\tau = 0$. Therefore, after the nondimensional total energy is defined as

$$\epsilon = \frac{u^2}{2} + \eta \tag{19}$$

the following result is obtained:

$$\epsilon = C_3 \tag{20}$$

If the end-conditions

$$u_i = \eta_i = 0 \quad , \quad \mu_i = 1 \tag{21}$$

$$u_f, \eta_f \equiv \text{given} \tag{22}$$

are considered and if

$$\zeta = 1 - \mu_f \tag{23}$$

denotes the unknown propellant mass ratio, the evaluation of the integration constants yields the following expression for the burnout conditions:

$$u_c = - \log (1-\zeta) - \frac{\zeta}{\tau_i} \tag{24}$$

$$\eta_c = \frac{1}{\tau_i}\left[\zeta + (1-\zeta) \log (1-\zeta)\right] - \frac{\zeta^2}{2\tau_i^2} \tag{25}$$

Consequently, use of Eq. (19) allows one to determine the burnout energy level ϵ_c, which in turn is identical with the energy level at the end of coasting ϵ_f. As a final result, the propellant consumed during take-off and the final energy level satisfy the relationship

$$\epsilon_f = \frac{1}{2} \log^2 (1-\zeta) + \frac{1}{\tau_i}\left[\zeta + \log (1-\zeta)\right] \tag{26}$$

which is plotted in Fig. 6. The associated burnout conditions are given in Figs. 7 and 8 in terms of the final energy level and the initial thrust-to-weight ratio.

In order to show that the constant thrust-zero thrust program is actually the best, it is useful to compare it with an arbitrary thrust program, for example, the thrust program which yields constant acceleration

during powered flight(*) followed by zero thrust. Consequently, if the equations of motion are integrated subject to the condition $\tau = \tau_i$, the propellant mass ratio is given by

$$\zeta = 1 - \exp\left[-\sqrt{\frac{2\tau_i\, \epsilon_f}{\tau_i - 1}}\right] \tag{27}$$

and is plotted in Fig. 9 versus the initial thrust-to-weight ratio for $\epsilon_f = 0.3$. Obviously, the constant thrust-zero thrust program is the better of the two. For example, if $\tau_i = 2$, the constant acceleration-zero thrust program requires 7% more propellant than the optimum thrust program.

5.5. Landing

If the nondimensional variables (12) are used, the differential equations for landing can be written in the form

$$\frac{d\eta}{d\theta} = -u \tag{28}$$

$$\frac{du}{d\theta} = -\tau + 1 \tag{29}$$

$$\frac{d\mu}{d\theta} = -\tau\mu \tag{30}$$

(*) Constant acceleration can be achieved by regulating the thrust in such a way that it is proportional to the mass of the vehicle at every time instant.

For the coasting subarc, Eq. (20) is still valid. On the other hand, for the subarc flown with maximum thrust, the thrust-to-weight ratio and the nondimensional mass satisfy the relationship

$$\tau = \frac{\tau_d}{\mu} \quad , \quad \tau_d = \frac{\beta_{max} V_E}{m_i g_o} \tag{31}$$

so that the integration process leads to

$$u - \log \mu + \frac{\mu}{\tau_d} = C_1 \tag{32}$$

$$\eta + \frac{\mu}{\tau_d} (1 - C_1 - \log \mu) + \frac{\mu^2}{2\tau_d^2} = C_2 \tag{33}$$

If the integration constants are evaluated for end-conditions

$$u_i, \eta_i \equiv \text{given} \quad , \quad \mu_i = 1 \tag{34}$$

$$u_f = \eta_f = 0 \tag{35}$$

the following relationship can be determined between the coordinates of the firing point, the thrust-to-weight ratio at the beginning of firing, and the propellant mass ratio

$$u_d = - \log (1-\zeta) - \frac{\zeta}{\tau_d} \tag{36}$$

$$\eta_d = - \frac{1}{\tau_d} \left[\zeta + \log (1-\zeta) \right] - \frac{\zeta^2}{2\tau_d^2} \tag{37}$$

and, in consideration of the coasting flight equation (20), imply that

$$\epsilon_i = \frac{1}{2} \log^2 (1-\zeta) - \frac{1}{\tau_d} \left[\zeta + (1-\zeta) \log (1-\zeta) \right] \tag{38}$$

This relation enables one to determine the propellant mass ratio required to land the vehicle in terms of the initial energy level and thrust-to-weight ratio and is plotted in Fig. 10. The corresponding firing conditions are indicated in Figs. 11 and 12 in terms of the initial energy level and the thrust-to-weight ratio. Finally, Fig. 13 shows a comparison of the zero thrust-constant thrust program and the zero thrust-constant deceleration program for the particular case where $\epsilon_i = 0.3$. The expression for the propellant consumed during the constant deceleration maneuver is given by Eq. (27), providing τ_i and ϵ_f are replaced by τ_d and ϵ_i, respectively.

4. VERTICAL FLIGHT IN AN INVERSE SQUARE LAW GRAVITATIONAL FIELD

In this section, the uniform gravitational field is replaced by one which is central and obeys the inverse square law

$$g = g_o \left(\frac{r_o}{r_o + h} \right)^2 \tag{39}$$

where g_o and r_o denote the acceleration of gravity at the surface of the attracting body and the radius of the attracting body, respectively. If it is assumed that Newton's law is valid for a reference frame rigidly associated with the attracting body, the equations of motion for ascending and descending vertical flight are given by

$$\frac{dh}{dt} = \pm V \tag{40}$$

$$\frac{dV}{dt} = \pm \frac{\beta V_E}{m} \mp g_o \left(\frac{r_o}{r_o + h} \right)^2 \tag{41}$$

$$\frac{dm}{dt} = - \beta \tag{42}$$

Since this set of differential equations has one degree of freedom, some optimum requirement can be imposed on the flight path. Again, it is desired that the burning program $\beta(t)$ be such that the propellant consumed during take-off or landing is a minimum. However, the choice of a program is still limited by the inequality constraint (6). From the equations of motion it is seen that the propellant required to transfer the vehicle from an initial state V_i, h_i to a final state V_f, h_f is given by the linear integral

$$\log (1-\zeta) = \int_i^f \left[\mp \frac{dV}{V_E} \mp \frac{g_o}{V_E V} \left(\frac{r_o}{r_o+h} \right)^2 dh \right] \tag{43}$$

Hence, the particular path h(V) which minimizes the propellant consumption maximizes the integral (43).

In a manner similar to that used in Section 3, it can be shown that the class of admissible displacements from a point and that to a point are bounded by the displacements $\beta = 0$ and $\beta = \beta_{max}$. Furthermore, the region of admissible paths is bounded by the $\beta = 0$ and $\beta = \beta_{max}$ curves which originate at the initial point and arrive at the final point. In view of the above statements, this problem meets all the requirements of a linear problem, so that the fundamental function is given by

$$\omega(V,h) = \pm \frac{g_o}{V_E V^2} \left(\frac{r_o}{r_o+h} \right)^2 \tag{44}$$

and, therefore, is positive for ascending flight and negative for descending flight. Consequently, the maximum thrust subarc precedes the coasting subarc for ascending flight and follows it for descending flight.

4.1. Take-Off

In order to study the main characteristics of the extremal arc for take-off, it is convenient to introduce the nondimensional variables

$$\eta = \frac{h}{r_o} \quad , \quad u = \frac{V}{\sqrt{g_o r_o}} \quad , \quad \theta = t\sqrt{\frac{g_o}{r_o}}$$

$$\mu = \frac{m}{m_i} \quad , \quad \tau = \frac{\beta V_E}{m g_o} \quad , \quad u_E = \frac{V_E}{\sqrt{g_o r_o}} \tag{45}$$

and rewrite the equations of motion as

$$\frac{d\eta}{d\theta} = u \tag{46}$$

$$\frac{du}{d\theta} = \tau - \frac{1}{(1+\eta)^2} \tag{47}$$

$$\frac{d\mu}{d\theta} = -\frac{\tau\mu}{u_E} \tag{48}$$

which, following the elimination of the time, imply that

$$\frac{d\eta}{d\mu} = -\frac{u_E u}{\tau\mu} \tag{49}$$

$$\frac{du}{d\mu} = \frac{u_E}{\tau\mu}\left[-\tau + \frac{1}{(1+\eta)^2}\right] \tag{50}$$

For the subarc flown with maximum thrust, these equations must be integrated numerically subject to the constraint (16). For the coasting subarc, the following result is obtained:

$$\epsilon = \text{Const} \tag{51}$$

where

$$\epsilon = \frac{u^2}{2} - \frac{1}{1+\eta} \tag{52}$$

is the nondimensional total energy.

If the initial conditions (21) are assumed, the integration process relative to the maximum thrust subarc yields the parametric equations

$$u = u(u_E, \tau_i, \mu) \quad , \quad \eta = \eta(u_E, \tau_i, \mu) \tag{53}$$

which, for $\mu = 1 - \zeta$, enable one to determine the burnout velocity, the burnout altitude, and, therefore, the burnout energy ϵ_c. Since the burnout energy is identical with the energy at the end of coasting ϵ_f, the function $\zeta(u_E, \tau_i, \epsilon_f)$ can be calculated and is plotted in Fig. 14 for $u_E = 2$ (for take-off from the Moon, this corresponds to an equivalent exit velocity of 11,000 ft sec^{-1}). The corresponding burnout conditions are shown in Figs. 15 and 16. In these diagrams, the line $\epsilon_f = 0$ represents the minimum escape condition; consequently, it separates the region where the vehicle reaches a peak altitude and falls back to the attracting body from the region where the vehicle escapes. Finally, in Fig. 17, the optimum thrust program is compared with (a) the constant thrust per unit mass-zero thrust program, (b) the constant thrust per unit weight-zero thrust program, and (c) the constant acceleration-zero thrust program, assuming that $\epsilon_f = 0$ and $u_E = 2$ (see Appendix B).

4.2. Landing

If the dimensionless variables (45) are introduced, the equations of motion can be written as

$$\frac{d\eta}{d\theta} = -u \tag{54}$$

$$\frac{du}{d\theta} = -\tau + \frac{1}{(1+\eta)^2} \tag{55}$$

$$\frac{d\mu}{d\theta} = -\frac{\tau\mu}{u_E} \tag{56}$$

and imply that

$$\frac{d\eta}{d\mu} = \frac{u_E u}{\tau\mu} \tag{57}$$

$$\frac{du}{d\mu} = \frac{u_E}{\tau\mu}\left[\tau - \frac{1}{(1+\eta)^2}\right] \tag{58}$$

The most convenient way to integrate these equations is to proceed backwards from the final point. Thus, if $\tau = \tau_d/\mu$ denotes the thrust program during the powered phase, if the end-conditions (35) are assumed, and if $\zeta = 1 - \mu_f$ denotes the propellant mass ratio, the integration process for the maximum thrust subarc yields the parametric equations

$$u = u(u_E, \tau_d, \zeta, \mu) \quad , \quad \eta = \eta(u_E, \tau_d, \zeta, \mu) \tag{59}$$

which, for $\mu = 1$, enable one to determine the firing velocity and altitude and, therefore, the firing energy ϵ_d. Since the firing energy is identical with the energy at the beginning of coasting ϵ_i, the function $\zeta(u_E, \tau_d, \epsilon_i)$ can be calculated and is plotted in Fig. 18. The corresponding firing velocity and altitude are given in Figs. 19 and 20. Finally, in Fig. 21, the optimum thrust program is compared with (a) the zero thrust-constant thrust per unit mass program, (b) the zero thrust-constant thrust per unit weight program(*), and (c) the zero thrust-constant deceleration program, assuming $\epsilon_i = 0$ and $u_E = 2$ (see Appendix B).

(*) The results for this program are only presented for the case where the thrust decreases monotonically. This occurs when $\tau_d \geq 4.34$.

5. VERTICAL FLIGHT IN AN ARBITRARY GRAVITATIONAL FIELD

If the gravitational field is arbitrary, that is, if the function g(h) is arbitrarily specified, the fundamental function becomes

$$\omega(V,h) = \pm \frac{g(h)}{V_E V^2} \tag{60}$$

and, therefore, has a constant sign throughout the admissible domain as long as the sign of g(h) is constant. When this condition is satisfied, the results of the previous section relative to the composition of the extremal arc remain qualitatively unchanged.

CONCLUSIONS

In this paper the thrust programs for minimum propellant consumption during vertical take-off and landing maneuvers of a rocket vehicle in a vacuum were derived, first for the case of a uniform gravitational field, then for the inverse square law gravitational field. It was shown that, regardless of the mathematical form of the attracting force, the extremal arc for the take-off is composed of a maximum thrust subarc followed by a coasting subarc, and the extremal arc for landing is composed of a coasting subarc followed by a maximum thrust subarc.

REFERENCES

1. MIELE, A., "Application of Green's Theorem to the Extremization of Linear Integrals", Boeing Scientific Research Laboratories, Flight Sciences Laboratory TR No. 40, 1961.

2. MIELE, A., "Flight Mechanics, Volume 1: Theory of Flight Paths", Addison-Wesley Publishing Company, Reading, Massachusetts, 1962.

3. MIELE, A., "Flight Mechanics, Volume 2: Theory of Optimum Flight Paths", Addison-Wesley Publishing Company, Reading, Massachusetts (in preparation).

4. GRÖBNER, W. and HOFREITER, N., "Integraltafel", Springer-Verlag, Wien, 1961.

APPENDIX A

THE ADMISSIBLE DOMAIN

The optimization technique employed in this report is based on one main assumption: all of the admissible arcs are contained in a region bounded by a closed curve ICFDI which, for the problem under consideration, is formed by the subarcs $\beta = 0$ and $\beta = \beta_{max}$ departing from the initial point and arriving at the final point. This statement can be proved by considering an arbitrary path departing from the initial point which is consistent with the mass flow constraint (6) and showing that this path (a) cannot cross the boundaries IC or ID and (b) cannot reach the desired final point once it has crossed the boundaries CF or DF.

Concerning the first part of the proof, observe that the slope of any trajectory in the velocity-altitude plane is given by

$$\frac{dh}{dV} = \frac{V}{\beta V_E \sqrt{m} - g_o} \tag{A-1}$$

and that the corresponding slope in the kinetic energy-potential energy plane is

$$\frac{d(g_o h)}{d(V^2/2)} = \frac{1}{\beta V_E \sqrt{m g_o} - 1} \tag{A-2}$$

Also, consider two ascending paths departing from the initial point, that is the $\beta \leq \beta_{max}$ trajectory IM and the $\beta = \beta_{max}$ trajectory IC, and define corresponding points A_1, A_2 as the points reached after an equal time interval

(Fig. 22). Since the thrust-to-weight ratio at point A_1 is smaller than the thrust-to-weight ratio at point A_2, the slope in the energy plane calculated at point A_1 is greater than that calculated at point A_2. Clearly, then, these two paths do not intersect in the energy plane and, therefore, do not intersect in the velocity-altitude plane. By an analogous procedure, it can be shown that the arbitrary path IM can never cross the boundary ID.

For the second part of the proof, assume that the arbitrary path under consideration crosses the boundary of the admissible domain at point M, and calculate the difference of the propellant consumed along the path IM and along the path IDM. In logarithmic form, this difference is given by

$$\Delta \log (1-\zeta) = \left[\log (1-\zeta)\right]_{IM} - \left[\log (1-\zeta)\right]_{IDM} . \qquad (A-3)$$

and in the light of Eq. (8), can be rewritten as

$$\Delta \log (1-\zeta) = \oint_{IMDI} \left[- \frac{dV}{V_E} - \frac{g_o dh}{V_E V} \right] \qquad (A-4)$$

Consequently, the application of Green's theorem relative to the transformation of a line integral into a surface integral leads to

$$\Delta \log (1-\zeta) = \iint_{\gamma} \frac{g_o}{V_E V^2} \, dV \, dh \qquad (A-5$$

where γ denotes the region internal to the contour IMDI (Fig. 22). Since

the integrand is always positive, one concludes that

$$\Delta \log (1-\zeta) > 0 \qquad \text{(A-6)}$$

which proves that at point M the mass of the vehicle along the path IM is larger than the mass along the path IDM. Now, consider the two curves MG ($\beta \leq \beta_{max}$) and MF ($\beta = \beta_{max}$) departing from point M, and define corresponding points B_1 and B_2 as the points reached after an equal time interval. Since the thrust-to-weight ratio at point B_1 is smaller than the thrust-to-weight ratio at point B_2, the slope in the energy plane calculated at point B_1 is larger than the slope at point B_2. Consequently, these paths do not intersect in the energy plane and, therefore, do not intersect in the velocity-altitude plane, so that the final point can never be reached. By analogous reasoning, one can prove that, if an arbitrary trajectory crosses the boundary CF, the final point can never be reached.

APPENDIX B

ANALYSIS OF COMPARISON PROGRAMS

In order to demonstrate that the so-called optimum thrust programs yield a minimum value for the propellant consumption, it is appropriate to compare these solutions with those pertaining to a number of arbitrary programs. With reference to the case where the gravitational field is central, the equations pertaining to vertical flight can be written in the form

$$\frac{d\rho}{d\theta} = \pm u \tag{B-1}$$

$$\frac{du}{d\theta} = \pm \tau \mp \frac{1}{\rho^2} \tag{B-2}$$

$$\frac{d\mu}{d\theta} = -\frac{T\mu}{u_E} \tag{B-3}$$

where $\rho = 1 + \eta$ denotes the nondimensional distance from the center of attraction. Elimination of the time from these equations yields the relationships

$$\frac{du}{d\rho} = \frac{1}{u}\left[\tau - \frac{1}{\rho^2}\right] \tag{B-4}$$

$$\frac{d\mu}{d\rho} = \mp \frac{T\mu}{uu_E} \tag{B-5}$$

which, generally speaking, must be integrated simultaneously. However,

if the thrust program has the form

$$\tau = \tau(\rho) \tag{B-6}$$

these equations uncouple, in the sense that Eq. (B-4) yields the velocity distribution and Eq. (B-5), the propellant consumption.

After the nondimensional total energy is written as

$$\epsilon = \frac{u^2}{2} - \frac{1}{\rho} \tag{B-7}$$

Eq. (B-4) becomes

$$d\epsilon - \tau(\rho)\, d\rho = 0 \tag{B-8}$$

and admits the general integral

$$\epsilon - \int \tau(\rho)\, d\rho = \text{Const} \tag{B-9}$$

Furthermore, after the differential equation for the mass is written as

$$\frac{d\mu}{\mu} = \mp \frac{1}{u_E} \sqrt{\frac{\rho}{2(\epsilon\rho+1)}}\, d\epsilon \tag{B-10}$$

the propellant consumed between the initial point and the final point becomes

$$\zeta = 1 - \exp\left[-\frac{G}{u_E}\right] \tag{B-11}$$

where

$$G = \pm \frac{1}{\sqrt{2}} \int_{\epsilon_i}^{\epsilon_f} \sqrt{\frac{\rho}{\epsilon\rho + 1}}\, d\epsilon \qquad \text{(B-12)}$$

In conclusion, Eq. (B-9) along with the appropriate initial conditions yields the function $\rho(\epsilon)$. Once this function is known, Eqs. (B-11) and (B-12) determine the propellant consumed when transferring the vehicle from one energy level to another.

B.1. Take-Off

The take-off problem is now considered for the end-conditions

$$\rho_i = 1 \quad , \quad \epsilon_i = -1 \quad ; \quad \epsilon_f = 0 \qquad \text{(B-13)}$$

It is assumed that the thrust program consists of a powered phase followed by a coasting phase. With regard to the powered phase, the following particular cases are considered: constant thrust per unit mass, constant thrust per unit weight, and constant acceleration.

If the thrust per unit mass is constant, the thrust program is represented by

$$\tau = \tau_i \qquad \text{(B-14)}$$

Consequently, Eq. (B-9) is solved by

$$\rho = \frac{\epsilon + 1 + \tau_i}{\tau_i} \qquad \text{(B-15)}$$

and the G-function necessary to evaluate the propellant consumed becomes

$$G(\tau_i) = \sqrt{2\tau_i}\left[F(\varphi,k) - E(\varphi,k) + \frac{\sqrt{\tau_i + 1}}{\tau_i}\right] \tag{B-16}$$

The symbols F and E denote elliptic integrals of the first and second kind, respectively, whose argument φ and parameter k are given by

$$\varphi = \arcsin\frac{1}{\sqrt{\tau_i}} \quad , \quad k = \frac{1}{\sqrt{\tau_i}} \tag{B-17}$$

If the thrust per unit weight is constant, the thrust program is represented by

$$\tau = \frac{\tau_i}{\rho^2} \tag{B-18}$$

Consequently, Eq. (B-9) is solved by

$$\rho = \frac{\tau_i}{\tau_i - 1 - \epsilon} \tag{B-19}$$

and the G-function becomes

$$G(\tau_i) = \sqrt{\frac{2\tau_i}{\tau_i - 1}} \tag{B-20}$$

If the acceleration is constant, the thrust program is represented by

$$\tau = \alpha + \frac{1}{\rho^2} \quad , \quad \alpha = \tau_i - 1 \tag{B-21}$$

where α denotes the nondimensional acceleration. Consequently, Eq. (B-9) is solved by

$$\rho = \frac{1}{2\alpha}\left[\epsilon + \alpha + \sqrt{(\epsilon+\alpha)^2 + 4\alpha}\right] \tag{B-22}$$

and the G-function becomes

$$G(\tau_i) = \frac{1}{\sqrt{2\alpha}}\left[2\alpha\sqrt{\lambda} + \frac{\sqrt{\lambda}}{1+\lambda} + \arctan\sqrt{\lambda}\right] \tag{B-23}$$

where

$$\lambda = \frac{1}{2}\left[\sqrt{1 + 4/\alpha} - 1\right] \tag{B-24}$$

B.2. Landing

In a manner analogous to that used for the take-off problem, the landing problem can be investigated for the end-conditions

$$\epsilon_i = 0 \quad ; \quad \rho_f = 1 \quad , \quad \epsilon_f = -1 \tag{B-25}$$

It is assumed that the thrust program consists of a coasting phase followed by a powered phase flown with either constant thrust per unit mass, con-

stant thrust per unit weight, or constant deceleration. With particular regard to the propellant consumption, the G-function can be written as follows:

Constant thrust per unit mass

$$G(\tau_d) = \sqrt{2\tau_d}\left[F(\varphi,k) - E(\varphi,k) + \frac{\sqrt{\tau_d + 1}}{\tau_d}\right] \tag{B-26}$$

$$\varphi = \arcsin\frac{1}{\sqrt{\tau_d}} \quad , \quad k = \frac{1}{\sqrt{\tau_d}}$$

Constant thrust per unit weight

$$G(\tau_d) = \sqrt{1 + \sqrt{1 + 4/\tau_d}} \tag{B-27}$$

Constant deceleration

$$G(\tau_d) = \frac{1}{\sqrt{2\alpha}}\left[2\alpha\sqrt{\lambda} + \frac{\sqrt{\lambda}}{1+\lambda} + \arctan\sqrt{\lambda}\right]$$

$$\lambda = \frac{1}{2}\left[\sqrt{1 + 4/\alpha} - 1\right] \tag{B-28}$$

$$\alpha^3 + (4-\tau_d)\,\alpha^2 - 4\tau_d\alpha + \tau_d^2 = 0$$

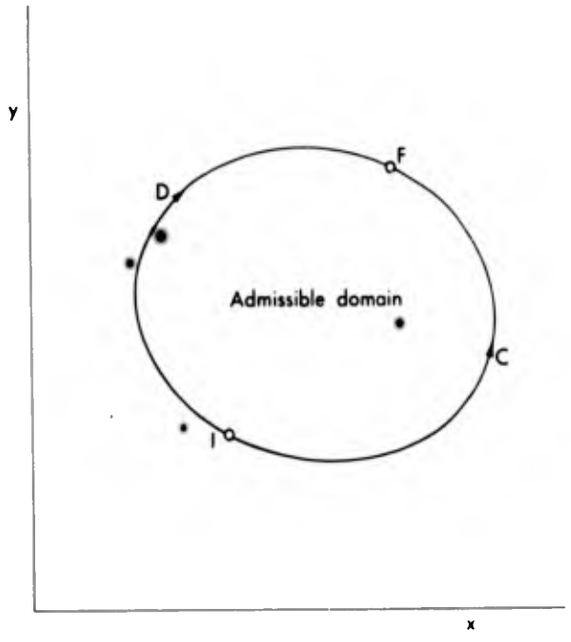

Fig. 1. Illustration for explanation of the theory.

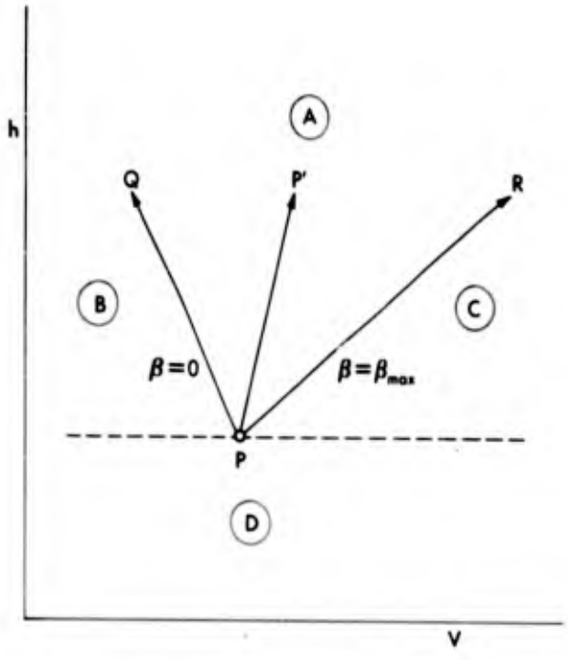

Fig. 2. Class of admissible displacements for ascending flight.

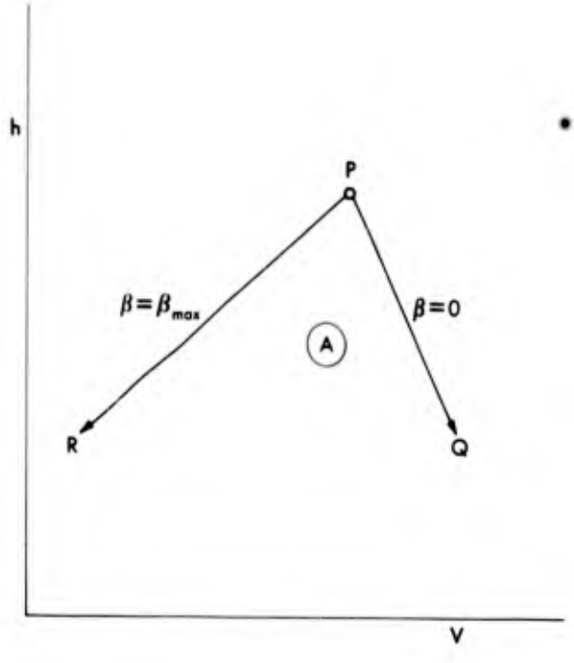

Fig. 3. Class of admissible displacements for descending flight.

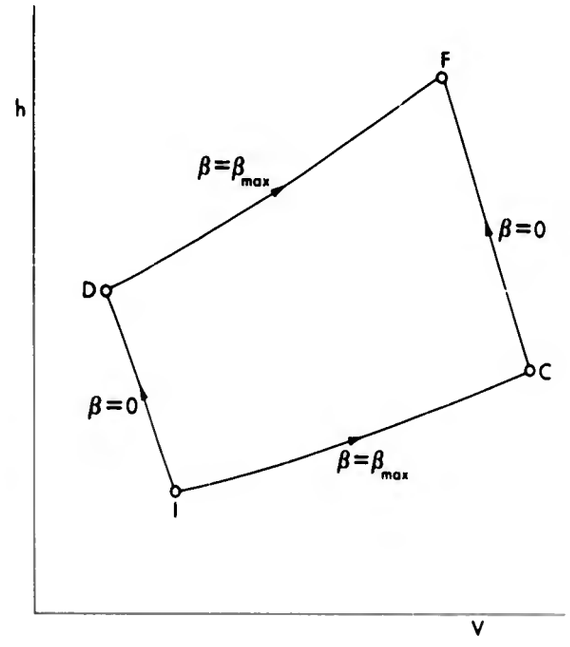

Fig. 4. Region of admissible paths for ascending flight.

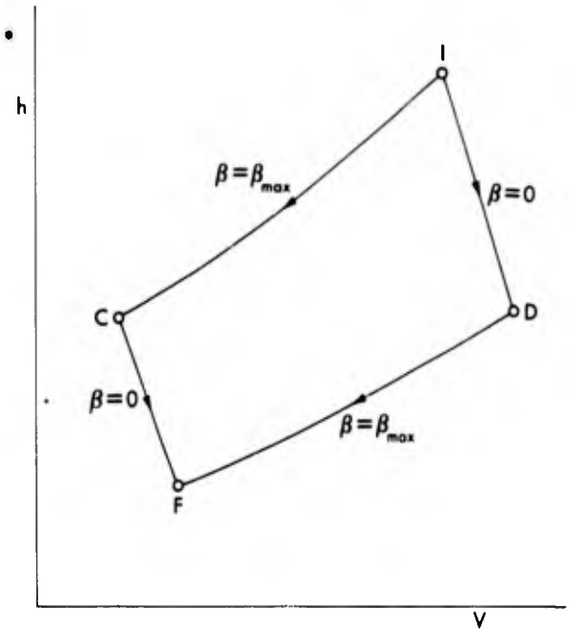

Fig. 5. Region of admissible paths for descending flight.

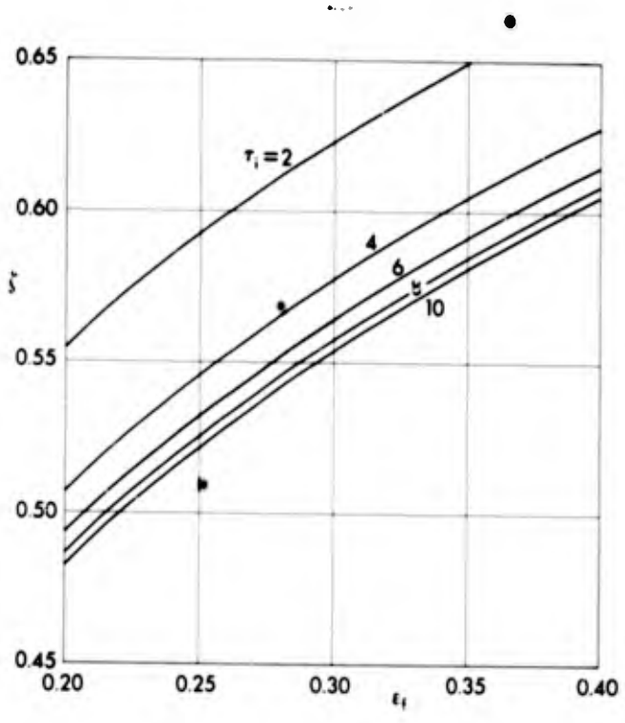

Fig. 6. Propellant required for take-off.

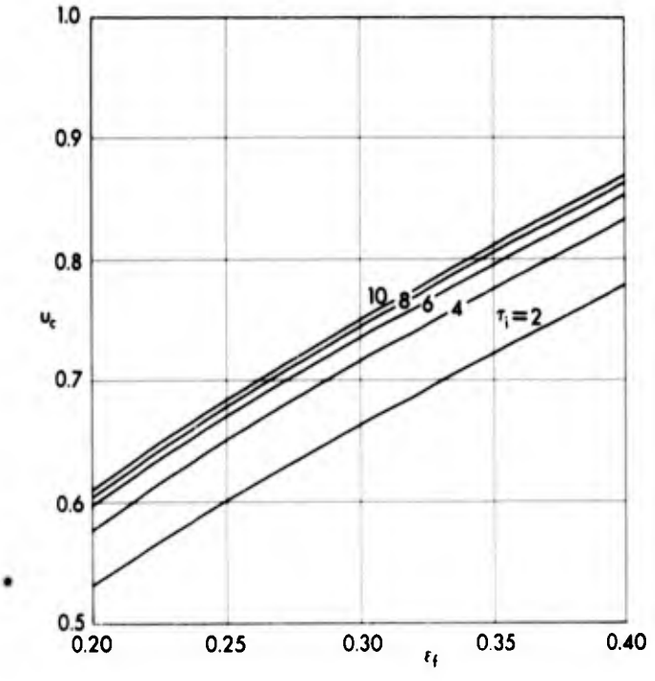

Fig. 7. Burnout velocity.

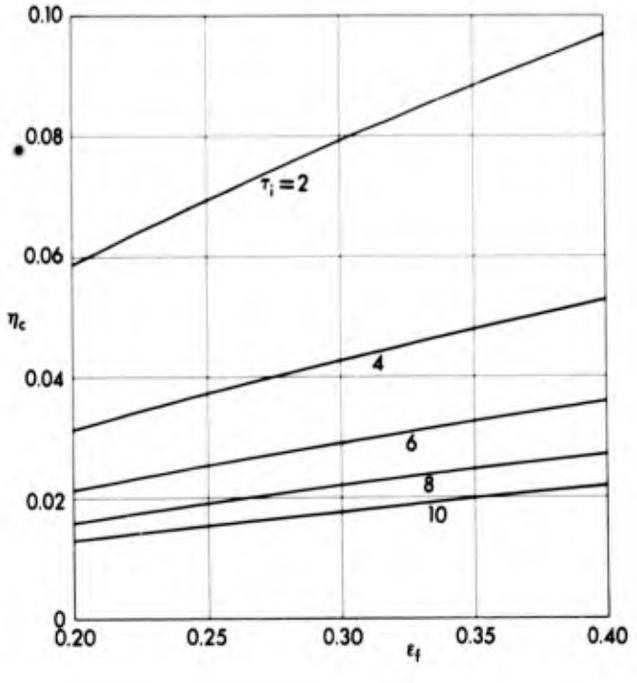

Fig. 8. Burnout altitude.

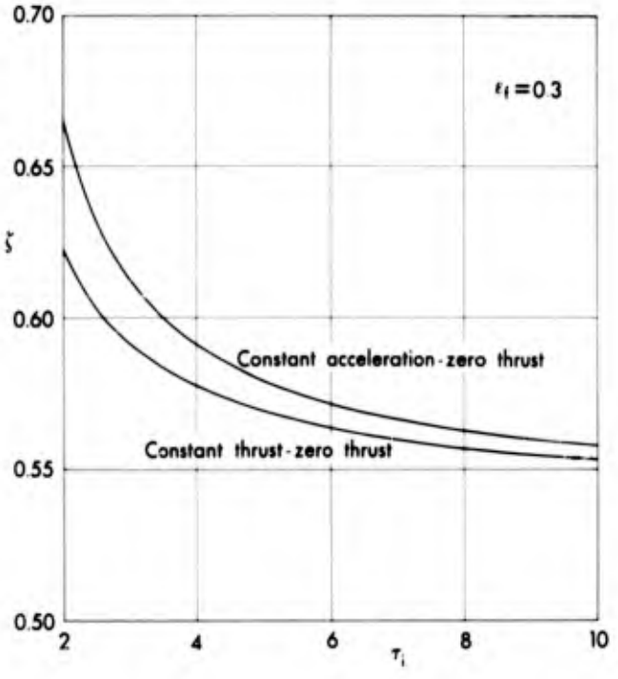

Fig. 9. Comparison of constant thrust and constant acceleration programs.

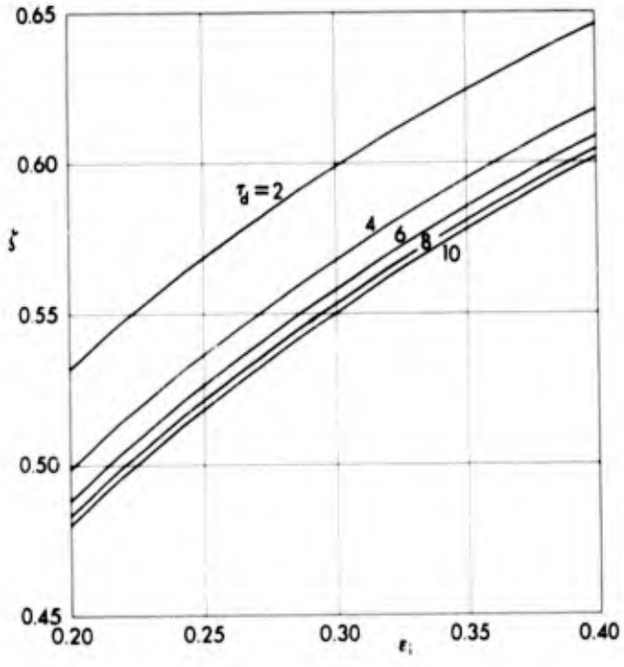

Fig. 10. Propellant required for soft-landing.

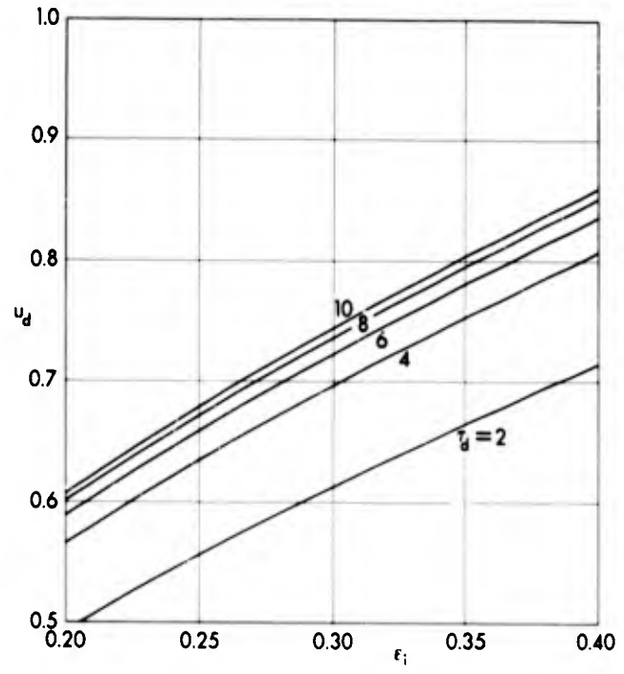

Fig. 11. Firing velocity.

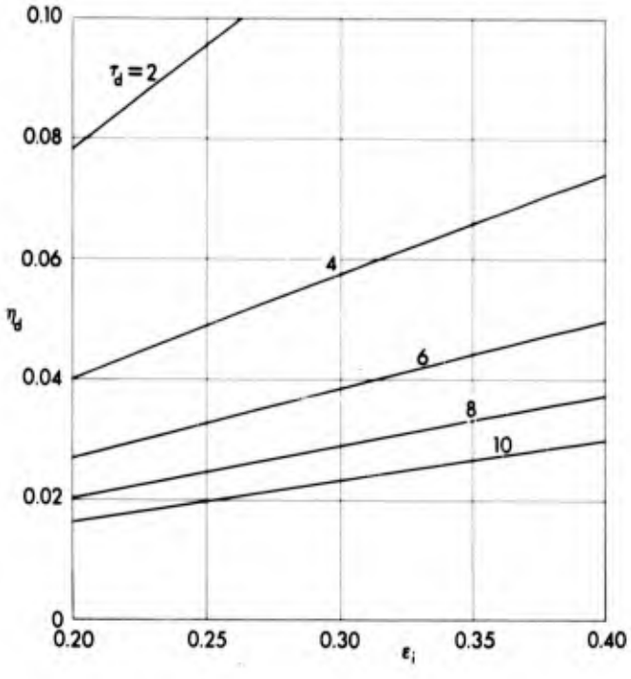

Fig. 12. Firing altitude.

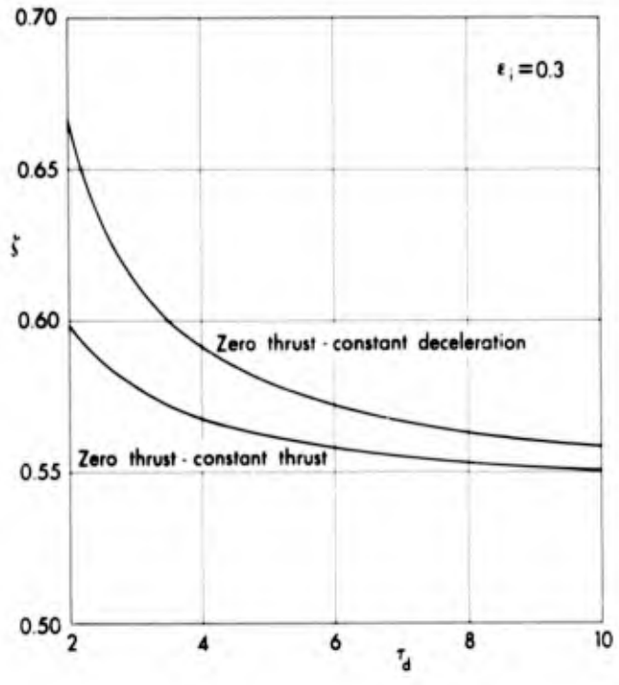

Fig. 13. Comparison of constant thrust and constant deceleration programs.

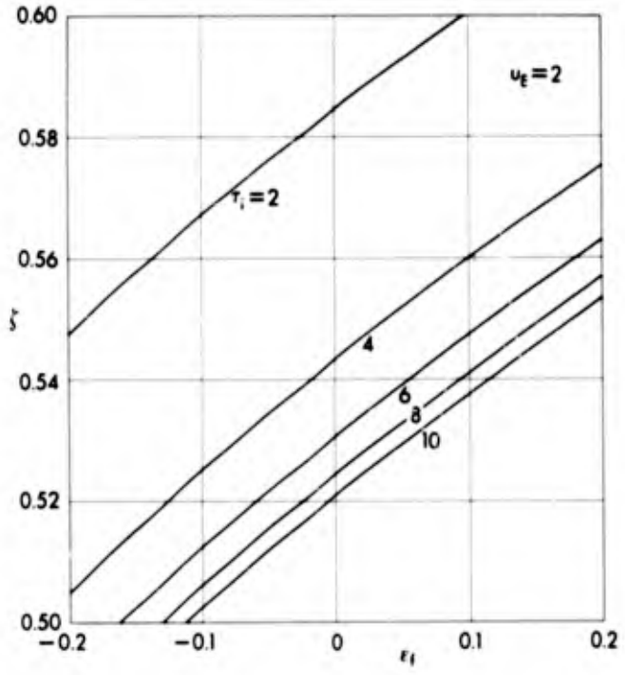

Fig. 14. Propellant required for take-off.

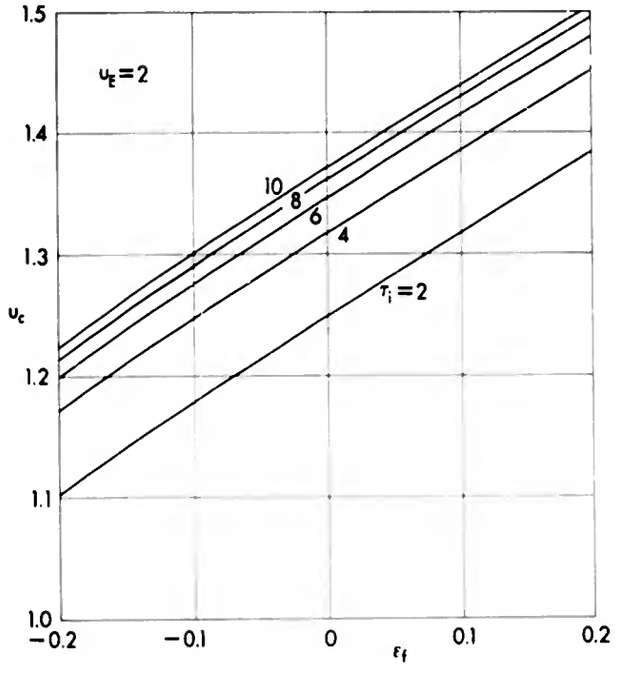

Fig. 15. Burnout velocity.

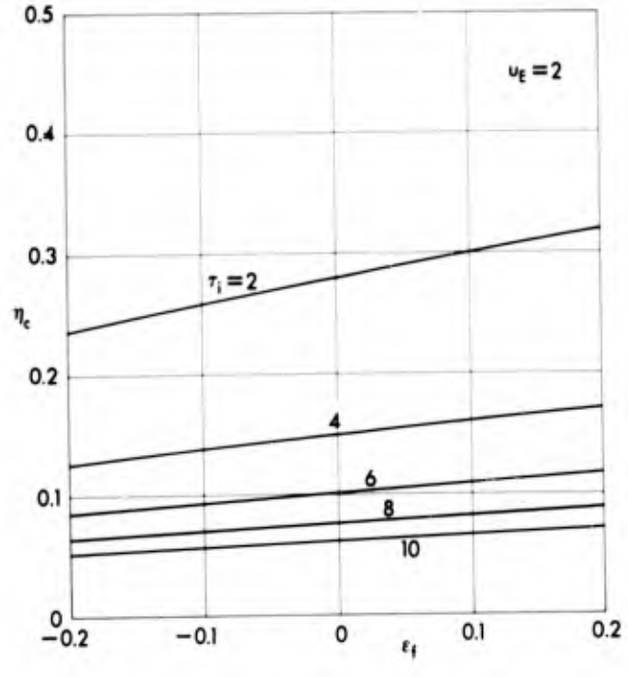

Fig. 16. Burnout altitude.

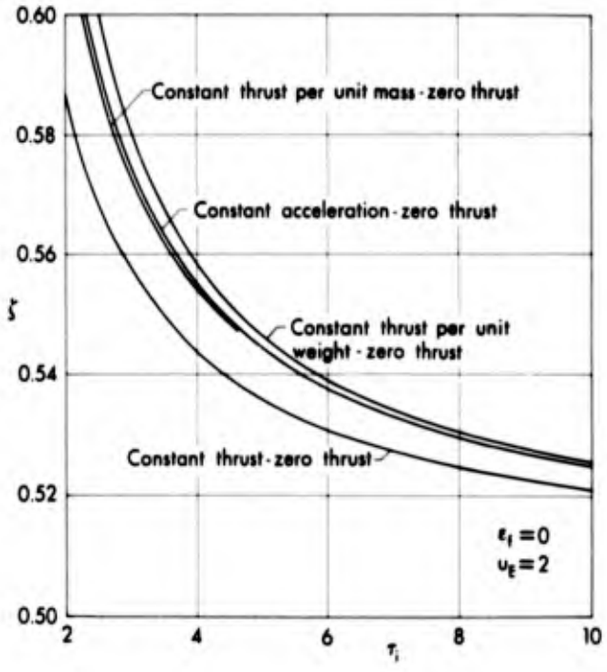

17. Comparison of optimum thrust program and several arbitrary programs.

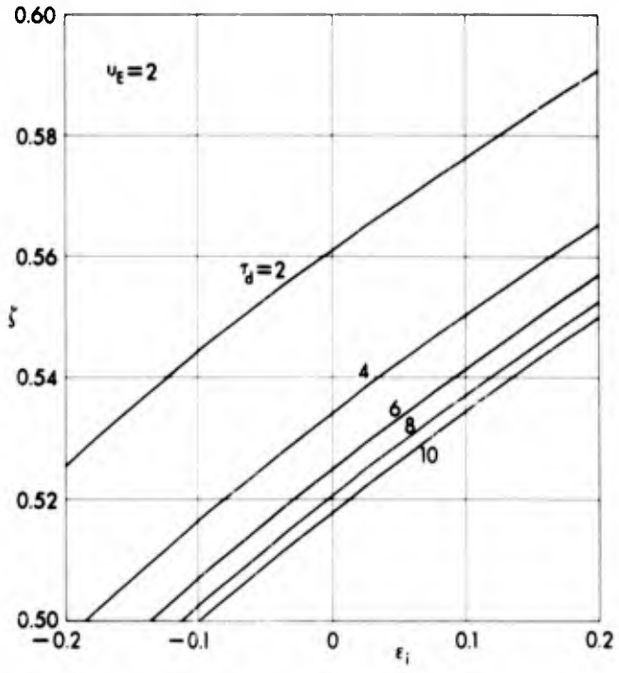

Fig. 18. Propellant required for soft landing.

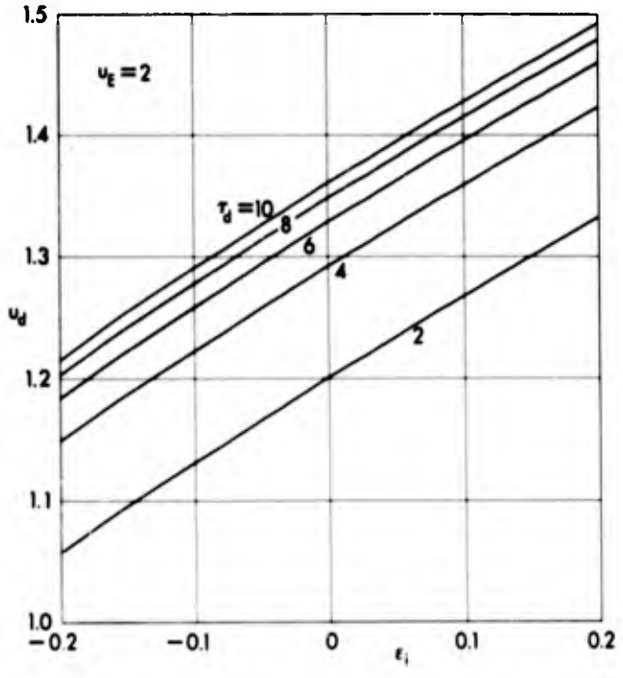

Fig. 19. Firing velocity.

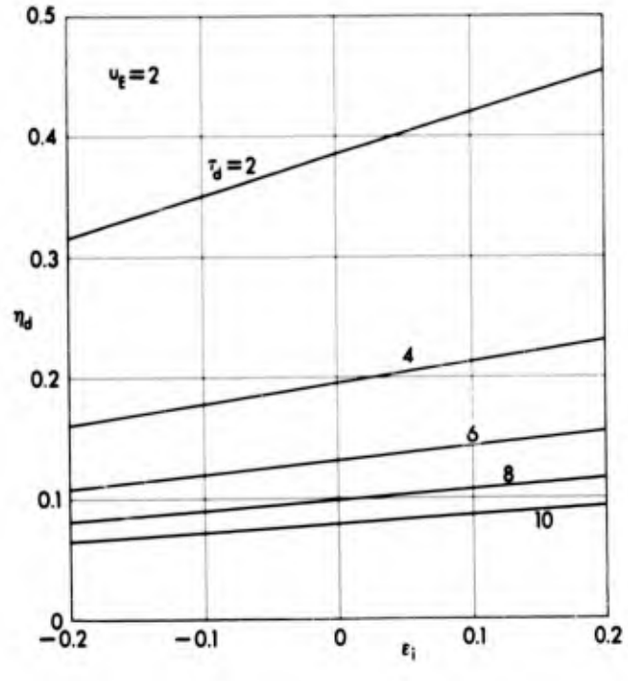

Fig. 20. Firing altitude.

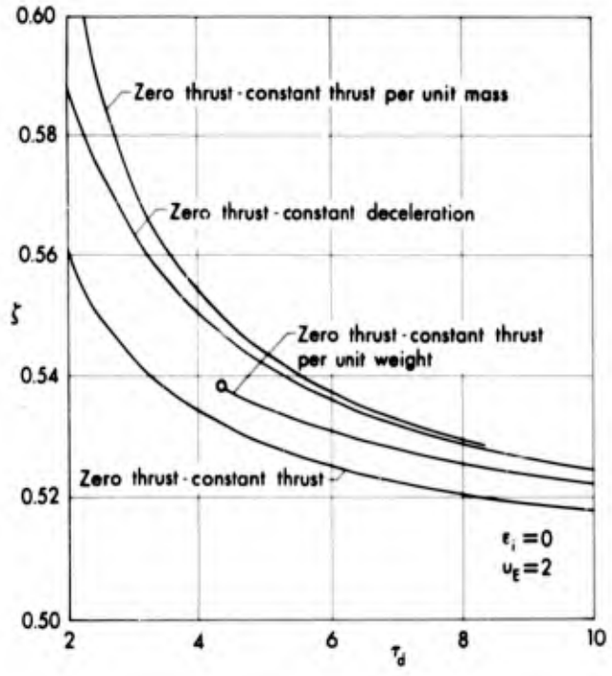

21. Comparison of optimum thrust program and several arbitrary programs.

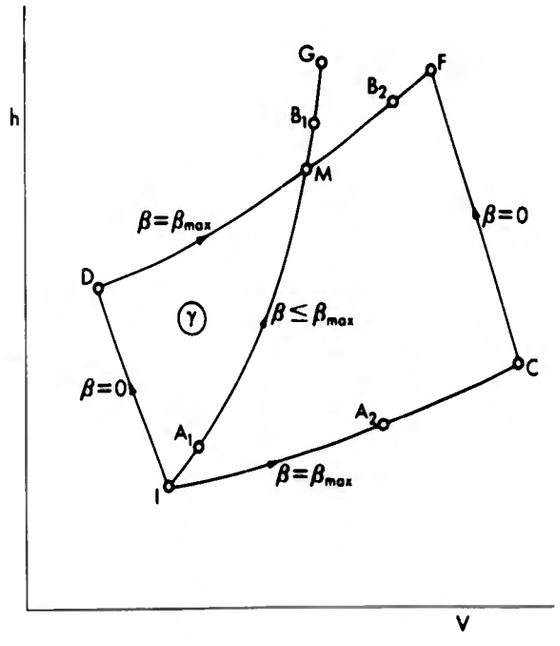

22. Illustration for the proof of the admissible domain.

UNCLASSIFIED